PCCP

PAPER

View Article Online
View Journal | View Issue

Cite this: *Phys. Chem. Chem. Phys.*, 2017, **19**, 25564

Surface modification induced enhanced CO_2 sorption in cucurbit[6]uril, an organic porous material†

Midhun Mohan,[a] T. Suzuki,[b] Akhil K. Nair,[ac] Saju Pillai,[a] K. G. K. Warrier,[a] U. S. Hareesh,*[a] Balagopal N. Nair*[bd] and J. D. Gale[d]

Received 9th June 2017,
Accepted 28th August 2017

DOI: 10.1039/c7cp03866f

rsc.li/pccp

The CO_2 adsorption properties of an organic macrocycle, cucurbit[6]uril (CB[6]), have been evaluated through experimental and theoretical studies. Quantum mechanical calculations show that CB[6] is capable of adsorbing the CO_2 molecule selectively within its cavity relative to nitrogen. Adsorption experiments at 298 K and at 1 bar pressure gave a CO_2 adsorption value of 1.23 mmol g^{-1} for the unmodified material. Significant enhancements in the CO_2 adsorption capacity of the material were experimentally demonstrated through surface modification using physical and chemical methods. Ethanolamine (EA) modified CB[6] provided an excellent sorption selectivity value of 121.4 for CO_2/N_2 at 323 K and is unique with respect to its discrimination potential between CO_2 and N_2. The chemical nature of the interaction between CO_2 and amine is shown to be the primary mechanism for the enhanced CO_2 absorption performance.

1. Introduction

The ever-increasing concentration of CO_2 in the Earth's atmosphere through gaseous waste emissions from the cement, iron and steel industries, as well as from thermal power plants, has necessitated substantial discussions on CO_2 separation, sequestration and reuse.[1–3] The selective adsorption of CO_2 from industrial gaseous wastes and flue gases, followed by its recycling/removal, is therefore a research topic of prime importance.[4–10] The inherent ability of amine solutions to capture CO_2 selectively from flue gas through the absorption between amine and CO_2 molecules is well established in the literature.[11–14] However, the handling and corrosion issues associated with the use of liquid amines and the loss of liquid amine at working temperatures remain the main drawbacks of these kinds of materials.[15–18] In addition, desorption of CO_2 from these materials is energy consuming and thus reinforces the high energy penalty for the CO_2 separation process.[19–21] Therefore, alternative approaches, such as physical and chemical adsorption on porous solids, have attracted attention as potential alternative solutions.

Recently, porous macrocyclic systems of both organic and inorganic origin have drawn a great deal of interest as promising candidates for molecular gas adsorption.[22–30] Cucurbit[*x*]uril, (CB), is an interesting organic macrocyclic system typically belonging to the class of porous organic materials, with exceptional properties suitable for potential applications in gas adsorption, host–guest chemistry and supramolecular complexation. The cavity of cucurbit[6]uril has nanoscale dimensions that position CB[6] as the most probable candidate among the CB[*x*] family for CO_2 adsorption.[31–37] The structure of CB[6] and its approximate cavity dimensions are shown in Fig. 1.

Owing to these favourable structural properties, the material has recently been explored as a prospective candidate for CO_2

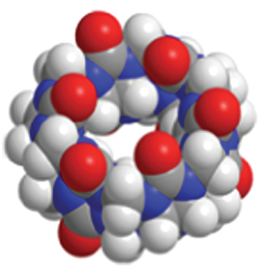

Cavity Dimensions	Size (Å)
Height	9.1
Outer Diameter	5.8
Inner Diameter	3.9

Fig. 1 Structure of Cucurbit[6]uril, $C_{36}H_{36}N_{24}O_{12}$ (carbon, nitrogen, oxygen and hydrogen are coloured dark grey, blue, red and light grey, respectively).

[a] *Functional Materials, Material Science and Technology Division, CSIR-National Institute for Interdisciplinary Science and Technology, Trivandrum-695 019, India. E-mail: hareesh@niist.res.in*
[b] *R&D Center, Noritake Co. Ltd, Miyoshi, Aichi, Japan. E-mail: bnair@n.noritake.co.jp*
[c] *Research and Postgraduate Department of Chemistry, Sree Vyasa N. S. S. College, Wadakkanchery, Kerala, India*
[d] *Curtin Institute for Computation, Department of Chemistry, Curtin University, PO Box U1987, Perth, WA 6845, Australia*
† Electronic supplementary information (ESI) available: See DOI: 10.1039/c7cp03866f

adsorption. For example, Kim and co-workers recently reported that CB[6] recrystallized from HCl showed high selective adsorption capacity towards CO_2 over CO at 298 K and 1 bar pressure.[38] It can therefore be anticipated that the modification of CB[6], either by chemical or physical means, provides an alternate option for the enhancement of the adsorption ability.[39,40] The high quadrupolar moment of CO_2 can be efficiently used for sequestration by logically employing a polar functional group with a high affinity towards CO_2 for modifying the pores of CB[6]. Such modifications will enhance the adsorption capacity as well as the selectivity for CO_2. However, Vaidhyanathan *et al.* demonstrated that a high degree of flexibility could lead to excessive clustering of amine groups thereby decreasing the adsorption capacity.[41] In this context, the proper incorporation of amine containing molecules on solid sorbents, such as CB[6] or its surface, would be a reasonable strategy to achieve a high performance CO_2 separation system with higher adsorption capacity.[42–47] Here, we have tried to understand the CO_2 adsorption properties of CB[6] through experimental and theoretical studies.[48,49] Later, we have attempted to improve the adsorption properties by modifying the material using physical and chemical means, ultimately realising modified materials with superior CO_2 absorption performance.

2. Experimental section

2.1 Materials

Cucurbit[6]uril (CB[6]) was purchased from Sigma Aldrich and used as received without any further purification (sample code CB[6]). H_2O_2 purchased from Merck India Pvt. Ltd, and ethanolamine (EA) purchased from SD Fine Chemicals Ltd were also used without further purification.

2.2 Synthesis of physically modified CB[6]

The physical modification of CB[6] was first explored by treating with H_2O_2. For this, 0.1 mmol of CB[6] was added to 10 mL of 30% H_2O_2 followed by sonication for a few minutes. The samples were filtered, dried and characterized using various spectroscopic techniques (sample code CB[6]-H_2O_2). Physical modification was also achieved by cryogenic grinding of the samples under liquid N_2 in an agate mortar (sample code CB[6]-liq. N_2). The modified samples were stored in air-tight sealed containers in all cases.

2.3 Synthesis of chemically modified CB[6]

The chemical modification of CB[6] particles was attempted by treating them with molecules having amine groups. We selected EA as the candidate for incorporating amine groups into the hydrophobic CB[6] cavity based on recent literature reports.[50–53] The solvo-thermal process of amine incorporation was carried out at 353 K for 8 h by taking 0.1 mmol of CB[6] and 5 mL of ethanolamine. The sample was further dried and characterized using various analytical and spectral techniques (sample code CB[6]-EA).

2.4 Characterization techniques

We evaluated the inherent CO_2 selective adsorption behaviour of CB[6] and modified CB[6] experimentally. Various microscopic and spectroscopic studies were conducted for the characterization. Scanning Electron Microscopy (SEM) analysis was performed using a JEOL JSM-5600LV Scanning Electron Microscope (tungsten source) with an accelerating voltage of 20 kV. Transmission Electron Micrographs (TEMs) of samples were recorded on a JEOL 3000EX TEM. Powder X-ray Diffraction (PXRD) analysis was performed on a XEUSS 2D SAXS/WAXS X-Ray diffractometer system operated at 50 kV and 0.6 mA. The source was Cu K_α radiation (λ = 1.54 Å). IR spectroscopic studies were carried out using an ALPHA-T BRUKER FT-IR spectrophotometer with a spectral resolution of ± 4 cm^{-1}. Volumetric CO_2 and N_2 adsorption experiments were performed using a BEL automatic gas sorption analyser (Belsorp max, BEL Japan INC). CO_2 and N_2 gas sorption was also measured gravimetrically at 323 K under flowing gas. A Perkin Elmer STA 6000 Thermogravimetric Analyser (TGA) was used to perform this measurement. For the measurement, about 10 mg of sample was initially loaded in the TGA sample pan. These samples were heated to 423 K under a He or N_2 gas flow of 30 mL min^{-1} to clean them of any adsorbed impurities. The temperature of the TGA was then decreased to 323 K and then the sweep gas was changed to the adsorbate gas of CO_2 or N_2. The increase in weight of the sample with time was measured and the amount adsorbed was calculated from it.

We also performed quantum mechanical energy minimizations to investigate the adsorption strength of CO_2 in CB[6] cavities. All such calculations were performed within the framework of Kohn–Sham density functional theory as implemented in the Quickstep module of CP2K.[54] Here, the nuclei and core electrons are described using the pseudo potentials of Goedecker, Teter and Hutter while the valence orbitals were expanded in a triple-zeta, doubly polarized (TZ2P) basis set.[55] An auxiliary plane wave basis set was used for calculating the density with a 400 Ry cut-off. The reason that pseudopotentials were used even for light elements is because the algorithm employed is the Gaussian Plane Wave technique that underpins CP2K. In this approach, the electron density is expanded in an auxiliary basis set of plane waves for the solution of Poisson's equation and therefore to reduce the cutoff of this basis, it is more efficient to replace the 1s core electrons (or smooth them as in the case of hydrogen). This is a standard feature of the method in CP2K, as well as other codes such as SIESTA that use an auxiliary grid for the electron density. The exchange–correlation functional of Perdew, Burke and Ernzerhof (PBE) was used along with dispersion corrections using the D3 approach of Grimme *et al.*[56,57] While there are more elaborate functionals that could be chosen than PBE, the dominant contribution to binding in this physisorption system is the van der Waals term and therefore this choice of exchange–correlation functional should be adequate. For the weaker physisorption prevailing in this system, the bonds in the adsorbate and adsorbent are hardly perturbed and therefore zero point energy changes are not a significant contribution and yet are disproportionately expensive to compute since they

require finite differencing of the forces over the entire system. This could also make the computations more susceptible to numerical noise and therefore they were not considered in our study. All binding energies in the calculations were corrected for basis set superposition error using a counterpoise correction.

3. Results and discussion

Firstly, SEM and TEM analyses were performed to understand the morphological properties of CB[6] before modification. The SEM images revealed that the particles possess a rod-like morphology with a length in the range of 2–5 μm and width in the range of 100–300 nm (Fig. 2A). The rod-like morphology of the unmodified CB[6] is further evidenced by TEM analysis (Fig. 2B).

The unmodified CB[6] sample was further characterized using FTIR and XRD analyses (Fig. 3A and B). The X-ray diffraction analysis indicated that CB[6] has an analogous characteristic structural pattern in the solid state as reported in the literature.[58] FTIR analysis indicated peaks corresponding to 1722 and 3518 cm^{-1}, which clearly confirmed the presence of carbonyl stretching and CO–N vibrations, respectively.

To have a better understanding of the pore structure, we examined the gas adsorption behaviour of the unmodified CB[6] powder samples. The temperature for cleaning pre-treatment (de-gassing) before the gas adsorption was selected based on the weight loss profile of the sample during heating as shown in the TGA analysis (Fig. S1, ESI†). The TGA profile clearly showed four different weight loss patterns in the temperature regimes of RT–120 °C (3.6% loss), 120–330 °C (2.23%), 330–490 °C (54.27%) and finally 490 °C to the measured maximum temperature of 600 °C (11.98%). Based on the TGA results, samples were de-gassed at 150 °C for 2 h prior to N_2 adsorption measurements at 77 K.

N_2 adsorption isotherms of the unmodified sample at 77 K (Fig. S2, ESI†) showed a Type III isotherm, representative of gas adsorption on the surface, indicating a very restricted entry of N_2 molecules into CB[6] pores under measurement conditions. As a result, the available porosity of the sample was very limited (0.032 cc g^{-1}), which is further reflected in the low surface area value of 9.3 m^2 g^{-1} calculated from the adsorption data of the sample.

N_2 adsorption measurements at 323 K also showed a similar type of isotherm, revealing an adsorption capacity of 1.63 cc g^{-1} (0.073 mmol g^{-1}) for N_2 at 100 kPa pressure (Fig. 4). However, the CO_2 adsorption isotherms clearly indicated adsorption typical of porous materials with maximum adsorption values of 27.5 cc g^{-1} (1.23 mmol g^{-1}) at 298 K and 9.36 cc g^{-1} (0.42 mmol g^{-1}) at 323 K (Fig. 4). CO_2/N_2 adsorption selectivity at 323 K can be calculated as 5.75 from this adsorption data.

Further, gravimetric adsorption capacity measurements were carried out in a TGA as explained earlier. Samples were heated to 423 K under a gas flow of 30 mL min^{-1} to clean them of any adsorbed impurities. The TGA profile of the sample

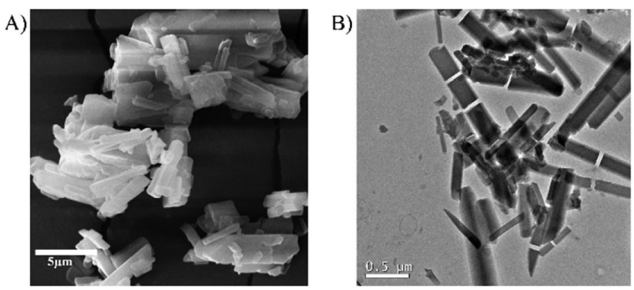

Fig. 2 (A) SEM and (B) TEM images of unmodified CB[6].

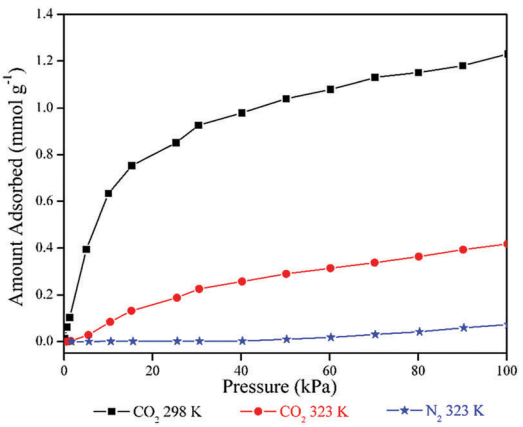

Fig. 4 CO_2 adsorption isotherm of unmodified CB[6] at 298 K and 323 K, N_2 adsorption isotherm at 323 K.

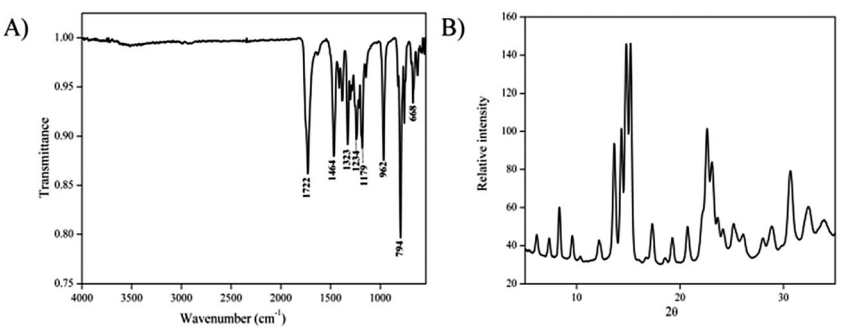

Fig. 3 (A) FT-IR and (B) XRD of unmodified CB[6].

(Fig. S3, ESI†) evidenced a ~5% weight reduction during the cleaning step. However, the sample weight remained stable after the initial reduction indicating that all of the physically adsorbed impurities were successfully removed before the adsorption step. CO_2 and N_2 adsorption capacity values at 323 K after 60 minutes of adsorption were measured as 0.54 mmol g^{-1} and 0.06 mmol g^{-1} using the gravimetric measurement. CO_2/N_2 adsorption selectivity at 323 K can be calculated as 9 from this adsorption data, which reasonably agrees with the adsorption selectivity value calculated using the volumetric adsorption method.

We used quantum mechanical calculations to investigate the strength of adsorption (and selective adsorption) of CO_2 in the CB[6] cavities. In particular, we considered the binding of CO_2, H_2O and N_2 on and in CB[6]. Starting with CO_2, we considered 9 distinct initial starting geometries as the basis for energy minimization in order to probe different binding modes (final optimized configurations are provided in the ESI†). Three binding configurations were found where CO_2 was on the outer surface of CB[6] with binding energies spanning 6.7 to 11.1 kJ mol^{-1}. These geometries involved the oxygen atoms of carbon dioxide being directed towards hydrogen atoms of both CH and CH_2 groups at distances of 2.5–2.8 Å. In the most favourable state (11.1 kJ mol^{-1}), the CO_2 molecule bridges hydrogen of both CH and CH_2 groups such that there is also a comparable distance of 2.6 Å from a further CH group to the carbon of the adsorbate.

A local minimum was also identified when the carbon of CO_2 lies approximately in the plane of the oxygen atoms of the carbonyl groups around the pore opening to CB[6] with the molecular axis tilted at approximately 30° to the principal axis of the host molecule. This leads to stronger binding than in the hydrocarbon regions of the external surface with a value of 31 kJ mol^{-1}. However, the strongest adsorption sites are reserved for configurations within the centre of pore, in line with the force field results. The most stable configuration, shown in Fig. 5, is close to the centre of symmetry with CO_2 oriented such that its molecular axis lies in the plane of the pore. While the strongest binding energy is 40.0 kJ mol^{-1}, there appears to be several shallow minima within ambient thermal energy in the centre of the cavity, suggesting that carbon dioxide will be relatively mobile as it explores these states. Rotating CO_2 to a configuration where the molecular axis is close to parallel to the pore axis lowers the binding energy to 24 kJ mol^{-1}.

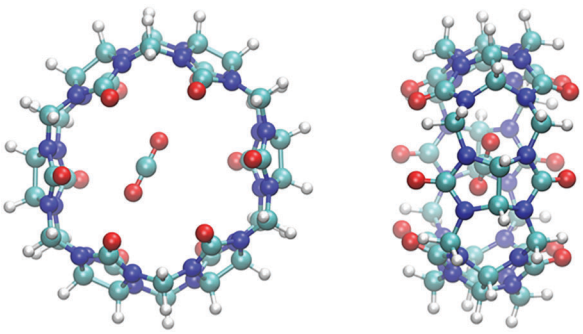

Fig. 5 Lowest internal energy configuration found for CO_2 binding in CB[6] at the PBE-D3 level of theory (front and side views).

Turning now to consider the adsorption of water on CB[6], a range of binding sites were identified through the quantum mechanical calculations. The first configuration examined had water bridging two carbonyl oxygen atoms at the rim of the pore, with H···O distances of 2.03 and 2.16 Å, which had a binding energy of 33.2 kJ mol^{-1}. Starting from this minimum and rotating the water by 90° led to the most stable binding site identified with an exothermic binding energy of 42.7 kJ mol^{-1}. Interestingly, this configuration has longer distances between one of the hydrogen atoms of water and the same two carbonyl oxygen atoms of ~2.9 Å, while the remaining hydrogen of water is directed across the pore diameter (Fig. 6). Despite the seemingly longer binding contacts, this configuration appears to be preferred, presumably due to the change in alignment of the water dipole moment.

Several configurations were also explored for water in the cavity of CB[6], either close to the centre or with hydrogen of water directed towards nitrogen as the most electronegative element within this region. All energy minima were found to be isoenergetic within 1 kJ mol^{-1}, with a binding energy close to 32 kJ mol^{-1}.

Considering the results for CO_2 and H_2O together, it appears that the former has the stronger preference for binding in the cavity of CB[6], while water is more stable when coordinated around the pore opening. To examine the interaction between mixed adsorbates, we optimised two arrangements where water

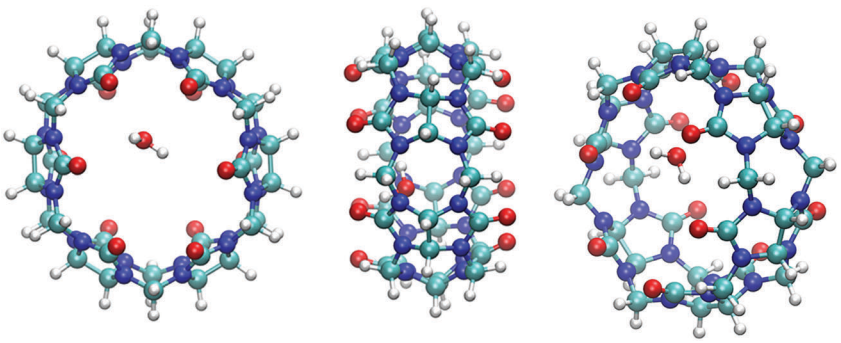

Fig. 6 Most stable binding geometry identified for water in CB[6] at the PBE-D3 level of theory (front, side and tilted views).

is in one of its favoured sites at the pore rim while carbon dioxide occupies the cavity. In both cases, the combined binding energies of CO_2 and H_2O at their equivalent sites alone were only reduced by an amount that is comparable to ambient thermal energy and the basis set superposition correction between the adsorbates. This indicates that there is neither a penalty nor cooperative enhancement of the binding strength of water and carbon dioxide when low loadings of both are present.

Lastly, for the computational part of this study we investigated the adsorption of N_2 in order to consider the competition for binding sites with CO_2. As would be expected, nitrogen only exhibits weak van der Waals adsorption on the outer surface of CB[6] with minima varying in binding energy from 5.5 to 10.8 kJ mol^{-1}. The less favourable binding strengths occur when N_2 is positioned over the hydrocarbon regions, while adsorption is slightly more favourable closer to the carbonyl groups. Within the centre of the cavity, nitrogen has a binding energy of 26 kJ mol^{-1} if the molecular axis lies diametrically across the pore, but is reduced to 17.8 kJ mol^{-1} if rotated to be at right angles to this. Based on the relative binding energies of carbon dioxide and nitrogen within CB[6], there is a clear preference for the former with a selectivity ratio of 182 for the first molecule at 323 K, a temperature near which these adsorbents are to be employed for practical CO_2 separation applications. However, the calculations suggest that the binding energy, and also therefore the selectivity, would rapidly decrease with increased loading since only a single molecule of CO_2 can adsorb strongly within the cavity at any given time. Furthermore, if binding in the cavity were to be partially hindered such that both CO_2 and N_2 were to be rotated parallel to the pore axis, then the selectivity for carbon dioxide over nitrogen would be reduced to 11.

As discussed previously, adsorption experiments at 298 K showed that the amount of CO_2 adsorbed at 100 kPa pressure is around 1.23 mmol g^{-1} or about 1.2 molecules of CO_2/molecule of CB[6] (molecular weight of CB[6] being 996.82). This value is reasonable when compared to other reported literature values of CB[6].[59] However, any further improvement in CO_2 adsorption capacity and selectivity to other molecules would be appreciated in view of the large flow rates of CO_2 in industrial flue gas streams. Hence, we tried to improve the adsorption properties of CB[6] by physical and chemical surface modifications. As explained in the Experimental section, the physically modified CB[6] samples were prepared by cryogenically grinding CB[6] powder in one case and treating with H_2O_2 in another instance. It should be noted that the treatment with H_2O_2 is considered as a physical modification here because we did not note any chemical changes in the modified material as will be discussed in the later part of this paper. It is possible that under much stronger reaction conditions, chemical changes may occur in CB[6] when treated with H_2O_2 or similar reagents. For the chemical modifications, we used EA molecules as explained in the experimental part. The selection of EA was based on the simplicity of the molecule for an easy understanding of the mechanism of adsorption. More importantly, we were concerned

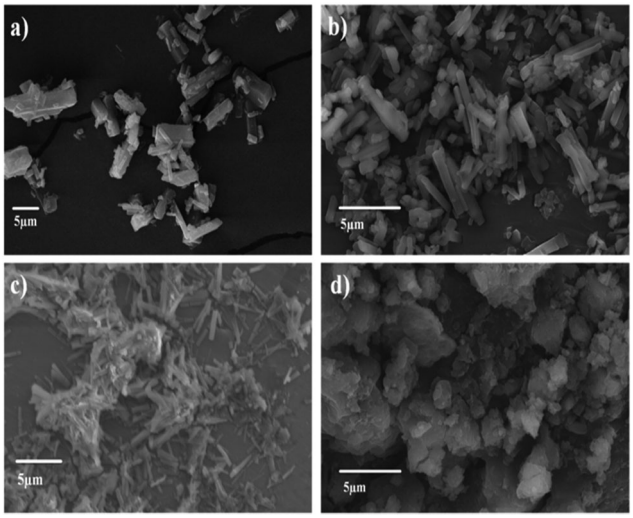

Fig. 7 SEM images of (a) CB[6], (b) CB[6]-H_2O_2, (c) CB[6]-liq.N_2 and (d) CB[6]-EA.

that the use of larger molecules such as ethylene diamine may cause steric issues within the limited space of CB[6] cavities and could lead to conflicting results even with minor changes in the conditions of study.[60,61] The characteristics of the modified materials are discussed in the following sections. We also performed gravimetric adsorption experiments at 323 K using CO_2 and N_2 molecules to evaluate the potential of the modified materials for practical CO_2 separation applications.

Firstly, in order to understand the morphological changes in CB[6] by the physical and chemical treatments, we carried out the SEM analysis of the samples. SEM images of both the unmodified (Fig. 7a) and treated samples are shown in Fig. 7b–d. The modification of CB[6] with H_2O_2 (Fig. 7b) obviously led to some degree of agglomeration of the powder particles. Cryogenic grinding of the samples (Fig. 7c) transformed the rigid rod shaped morphology of CB[6] to much smaller fragments. Fig. 7d shows the SEM microstructure of the samples that underwent incorporation of ethanolamine into the cavity of CB[6]. A significant change in the microstructure is visible in these samples.

All the samples were also characterized using FTIR and XRD techniques (Fig. 8 and 9). XRD analysis in Fig. 8B clearly indicated that no structural modifications were induced in the CB[6] samples before and after treatment with H_2O_2. Auxiliary confirmation obtained from the FTIR analysis (Fig. 8A) showed a typical CB[6] spectrum devoid of any chemical modification, at least to a level that could be detected by FTIR. The cryogenically ground samples also revealed no chemical or crystal structural changes.

However, the FTIR results of the ethanolamine incorporated samples showed the presence of amine peaks at 3299 cm^{-1}, indicating that the ethanolamine molecules were adsorbed inside the CB[6] cavity (Fig. 9A). From the XRD analysis it is clear that there has been a structural modification from the parent CB[6]. New peaks have appeared due to the presence of amines that are incorporated inside the cavity (Fig. 9B).

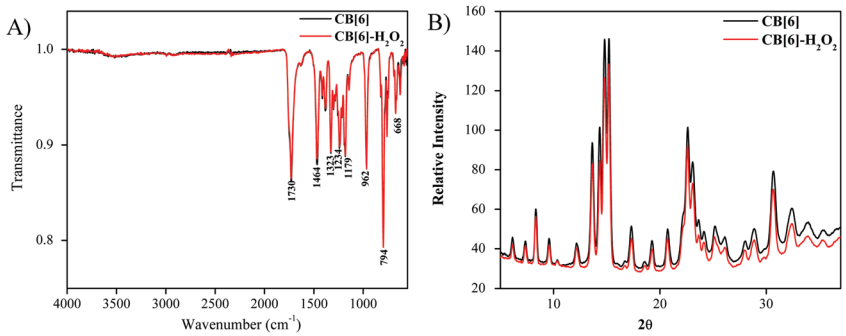

Fig. 8 (A) FT-IR and (B) XRD patterns of H_2O_2 treated CB[6] in comparison to unmodified CB[6].

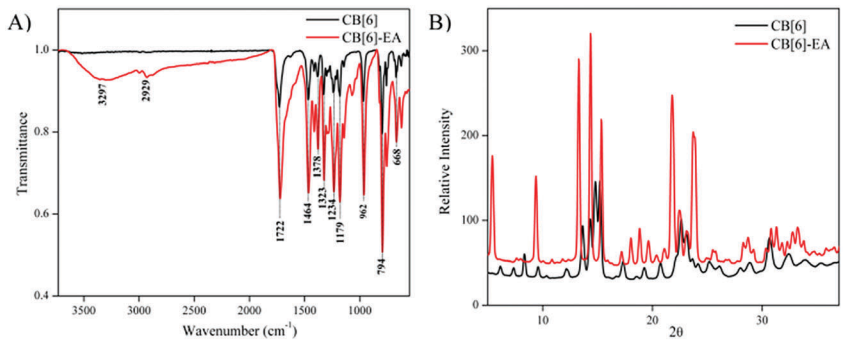

Fig. 9 (A) FTIR and (B) XRD of CB[6]-EA in comparison to unmodified CB[6].

FTIR, XRD and SEM analysis of the sample showed significant changes in CB[6] characteristics that clearly indicated that the incorporation of the amine molecule on CB[6] caused significant chemical and structural changes in the particles.

The gas adsorption behaviour of the CB[6] samples before and after surface modifications was therefore probed using N_2 and CO_2 sorption at 323 K. For the adsorption measurements, all the materials were heated to 423 K for 30 min to fully remove any adsorbed gas molecules in the sample before the gas sorption analysis as explained previously. The modified CB[6] samples were stable under these conditions, with no apparent loss of crystallinity. The adsorption was carried out at 323 K by flowing gas at the rate of 31 mL min^{-1} over the sample. The weight gain of the sample due to gas adsorption was tracked against time to obtain plots as shown in Fig. 10.

As shown, the adsorption plots of the samples were very different and signified the chemical and structural changes that took place during the modifications. The unmodified samples attained an adsorption saturation value of 0.54 mmol g^{-1} in ~30 min. Samples modified with H_2O_2 followed a much slower adsorption rate, but reached a larger adsorption value of 0.78 mmol g^{-1} within 60 min of adsorption measurement, as seen in Fig. 10. The adsorption saturation value in this case was calculated as 1.06 mmol g^{-1}. In the samples modified by H_2O_2, no significant chemical changes were observed compared to the unmodified sample in the FTIR or XRD analysis. Yet, the slow kinetics of adsorption here should be an indication of the changes in the surface structure of the CB[6] particles. As shown in the SEM images (Fig. 7b), H_2O_2 treatment did not alter the morphology of the particles significantly, as in the case of amine or cryogenic grinding treatment. Some amount of surface roughening of the CB[6] particles due to dissolution, leading to increased adsorption volume but slower adsorption rate, could be expected upon treatment with H_2O_2.

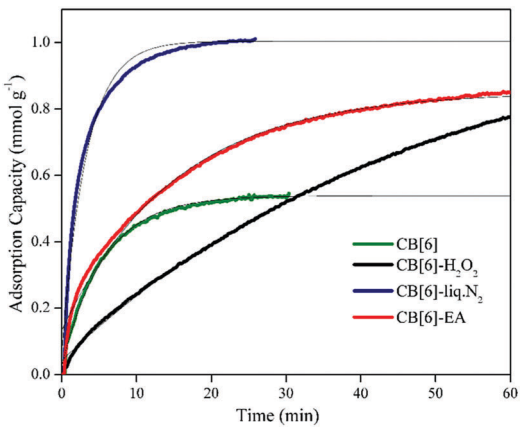

Fig. 10 Adsorption capacity of CO_2 in CB[6] before and after modifications. Adsorption temperature was 323 K and measurement method was gravimetric. 100% CO_2 gas was used. Experimental data, as well as fitted lines, are shown.

The cryogenically ground samples exhibited a completely different adsorption pattern. A much larger adsorption value of 1.04 mmol g^{-1} was achieved within the first 20 min of adsorption itself. It could be expected that the fragmentation of the particles during liq. N_2 assisted crushing helped to

expose many more cavities directly for CO_2 adsorption, which were possibly not available in the unmodified sample owing to the macro-particle nature of the commercial CB[6] material. Although CB[6] cavities are intrinsic and should be available for adsorption in all cases, the size of the particle could reduce adsorption due to diffusion limitations. Powdering and fragmentation can therefore help in achieving better adsorption performance for practical purposes, as is well supported by the SEM images (Fig. 7), which showed the smaller particle size for the cryogenically ground samples.

The sample treated with ethanolamine reached an adsorption capacity value of 0.85 mmol g^{-1} after 60 min of exposure to CO_2 at 323 K. The adsorption saturation value in this case was calculated as 0.93 mmol g^{-1} and the rate of adsorption was similar to that of the unmodified sample. However, the adsorption proceeded to attain much higher capacities than the unmodified sample. Compared to the physical modification approach, the maximum adsorption capacity of the EA modified sample was slightly lower.

N_2 adsorption measurement was extremely difficult and the quality of gravimetric isotherms was poor due to the very low adsorption capacity values and therefore only the adsorption value after 60 min of adsorption was extracted from the measurement. These adsorption capacity values of N_2 on CB[6] and the modified CB[6] samples measured at 323 K and 1 bar gas pressure are shown in Table 1. As a rough measure of selectivity, the ratio of adsorption capacity values of CO_2/N_2 is also listed in Table 1. From the results listed in Table 1, it is clear that the unmodified sample and the physically modified samples only provided limited selectivity for CO_2 against nitrogen. However, the ethanolamine modified samples provided an excellent sorption selectivity value of 121.4 for CO_2/N_2 at 323 K. The chemical nature of the interaction between CO_2 and amine is hence clear from the results.

We further confirmed the mechanism of adsorption of CO_2 in CB[6] and the modified CB[6] samples using FTIR analysis. The FTIR spectra of all the samples were taken before exposure to CO_2 gas (original material), after the exposure to CO_2 gas and after heating the sample to 423 K for the complete desorption of CO_2 (Fig. 11). After CO_2 adsorption, the FTIR of CB[6] and the modified CB[6] samples showed the characteristic CO_2 vibration peak around 2336 cm^{-1} thereby confirming that adsorption had occurred. After heating at 423 K, the FTIR patterns of the samples showed the disappearance of the peak at 2336 cm^{-1}, clearly confirming the CO_2 desorption. In the case of CB[6], CB[6]-H_2O_2 and CB[6]-liq.N_2, FTIR analysis evidenced only physical adsorption of the CO_2 molecule. However, in the case of the CB[6]-EA sample, the reaction of CO_2 with the amine occurs through a Zwitterion mechanism to form carbamates, a reaction that has been extensively studied.[62] The ammonium carbamate formation and the interaction of amine molecules with CO_2 are well demonstrated by FTIR observations.

The FTIR spectrum of the CB[6]-EA sample, as shown in Fig. 11D, showed a broad peak for the incorporated amine molecules at 3299 cm^{-1}. However, no chemical interaction between CB[6] and the amine could be evidenced from the results. It is expected that the amine molecules were placed in the CB[6] cavities by ethanolamine modification. CO_2 would have adsorbed to the amine end of ethanolamine as well as in the remaining CB[6] cavities. The FTIR results of the CO_2 absorbed samples indeed support this. On CO_2 gas exposure, broadening of the peak at 3299 cm^{-1} was visible, which indicated ammonium carbamate formation. The peak at 1557 cm^{-1} clearly supported the formation of ammonium carbamate in CB[6]-EA, which is not present in the other samples. Moreover, the absorption band at 1458 cm^{-1} (C–N stretching) showed a slight shift to the lower wavelength region confirming CO_2 adsorption to the amine moiety. As mentioned earlier, the peak at 2336 cm^{-1} clearly confirmed the presence of physical adsorption in the sample. Thus, in the case of the CB[6]-EA sample, CO_2 molecules were not only trapped in the cavities (physical adsorption) of CB[6], but also chemically bonded to amine molecules forming weak chemical bonds. However, the presence of amine molecules in the cavities should have reduced the available free cavity space for CO_2 adsorption and therefore no significant increase in adsorption capacity could be realised by this modification. Fig. 12 shows the CO_2 adsorption isotherms at 313 K, 323 K and 353 K for the CB[6]-EA samples as measured using the volumetric method. As in the case of the unmodified CB[6] samples, the measured adsorption value at 323 K is slightly smaller than the values measured using the gravimetric method, which could be due to the differences in conditions between the measurements. Comparison of data in Fig. 4 and 12 reveals that the effect of temperature on the amount of CO_2 adsorbed is less drastic in the amine modified sample compared to the unmodified sample. Our previous studies on CO_2 adsorption in amine functionalized microporous silica materials have shown a similar trend wherein the incorporation of amines helped to realize a less drastic drop in CO_2 adsorption with increases in adsorption temperatures.[44] However, the heat of adsorption values of the amine modified material and comparison to values reported in the literature gave a clearer picture of the possible mechanism of CO_2 adsorption. Calculated heat of adsorption for the CB[6]-EA sample was -37 kJ mol^{-1} (at 0.15 mmol g^{-1} CO_2 loading), which is smaller than the value of -48 to -90 kJ mol^{-1} reported in the literature for adsorption of CO_2 in amine-functionalized adsorbents.[63] This value, however, is higher than the heat of adsorption values of -30 to -33 kJ mol^{-1} reported for adsorption of CO_2 in CB[6] micropores.[38] These results point to an adsorption mechanism wherein part of the CO_2 gas molecules are adsorbed physically in the CB[6] pores and the remaining CO_2 molecules are attached to the amine end of EA molecules

Table 1 Adsorption capacity of CO_2 and N_2 (60 min at 323 K) as well as CO_2/N_2 ratio measured on CB[6] and modified CB[6] samples

	Adsorption capacity (mmol g^{-1})		
Samples	CO_2	N_2	$CO_2:N_2$ ratio
CB[6]	0.54	0.06	9.0
CB[6]-H_2O_2	0.78	0.15	5.2
CB[6]-liq.N_2	1.04	0.28	3.7
CB[6]-EA	0.85	0.007	121.4

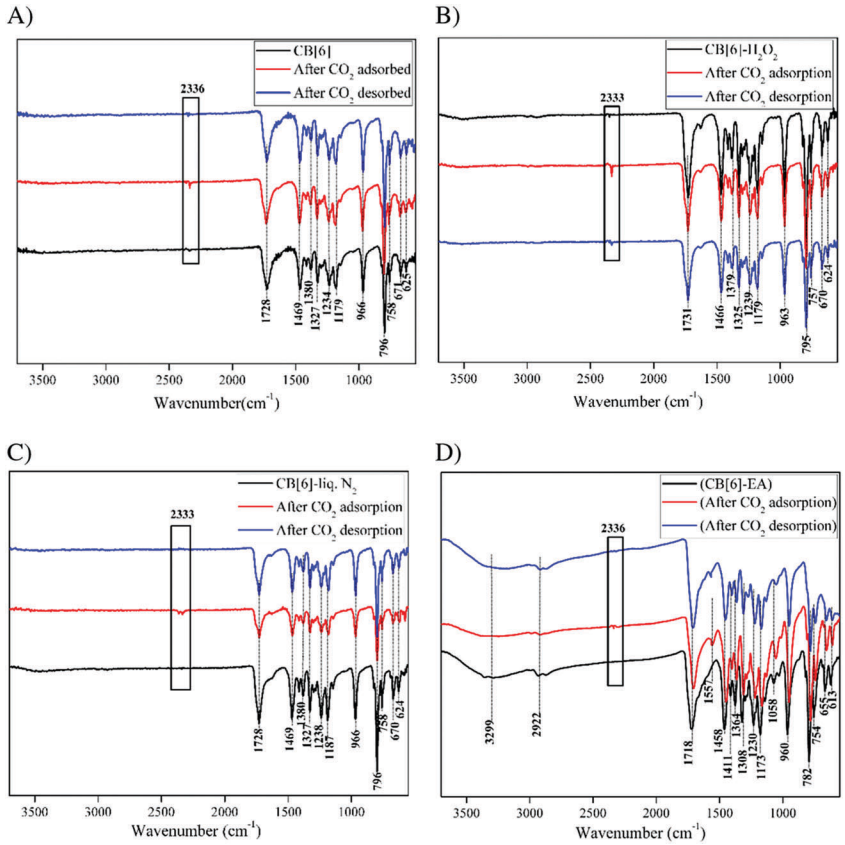

Fig. 11 (A) FTIR spectra of (–) CB[6], (–) after CO_2 adsorption and (–) after CO_2 desorption. (B) FTIR spectra of (–) CB[6]-H_2O_2, (–) after CO_2 adsorption and (–) after CO_2 desorption. (C) FTIR spectra of (–) CB[6]-liq.N_2, (–) after CO_2 adsorption and (–) after CO_2 desorption. (D) FTIR spectra of (–) CB[6]-EA, (–) after CO_2 adsorption and (–) after CO_2 desorption.

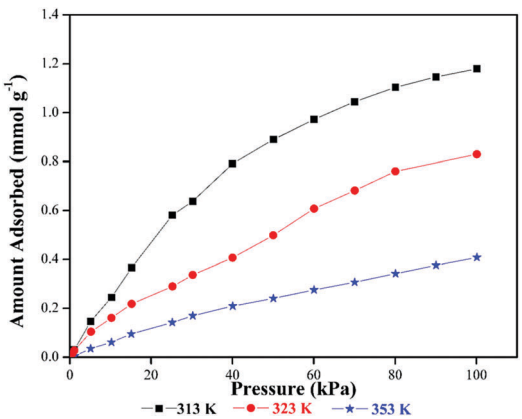

Fig. 12 CO_2 adsorption isotherm of CB[6]-EA at 313 K, 323 K and 353 K.

in the modified material as mentioned before. The reduction in the amount of N_2 adsorbed in the sample should be due to the fact that EA selectively occupied most of the available sites in the surface cavities, edges and pore-mouths of the material where CO_2 molecules tend to adsorb less selectively compared to N_2, thereby selectively reducing the amount of N_2 adsorbed in the modified material. Hence, the large CO_2/N_2 adsorption selectivity value measured for the CB[6]-EA sample, as shown in Table 1, can be well justified.

Even though it is very difficult to determine the exact nature of CO_2 sorption sites and mechanism of adsorption in the modified materials, we have obtained some insights based on the preliminary adsorption studies presented in this paper. Characterisation studies, especially FTIR, of the absorbed and desorbed samples helped us to understand the mechanism of CO_2 adsorption and desorption in these materials to some extent. NMR studies would have contributed more, however the low solubility of CB[6] in generally employed solvents has impeded such studies. Based on the present experimental and theoretical results, it can be concluded that the higher adsorption capacity of the surface treated CB[6] samples could be attributed to the availability of a larger amount of cavity when compared to the unmodified one. In the case of the amine incorporated samples, CO_2–amine interactions and poor N_2 adsorption in the amine rich sample as evidenced by the FTIR and CO_2/N_2 adsorption analysis should have contributed well to the resulting adsorption selectivity.

4. Conclusions

The mechanism of CO_2 adsorption in the organic macrocycle CB[6] has been studied and modifications based on physical and chemical treatments have been attempted. Quantum mechanical

calculations have shown that the binding energy for the adsorption of CO_2 in CB[6] is greater than that of N_2 and the estimated upper bound to selectivity within the cavity is consistent with the experimentally measured data. In addition, it was found that carbon dioxide will preferentially bind in the cavity of CB[6] relative to water, though H_2O can bind with a slightly more exothermic strength than CO_2 when it is situated in its preferred site close to the pore opening. While the loading of CO_2 in the cavity of CB[6] appears to be limited to a single molecule, at least close to the maximum binding energy, the co-adsorption of carbon dioxide and water appears to be possible with only a minimal effect on the individual thermodynamics due to the preference for different binding sites.

Experimental studies have shown that the material is capable of adsorbing 1.23 mmol g^{-1} of CO_2 at 298 K/100 kPa CO_2 pressure. Physical and chemical modifications achieved by various methods including H_2O_2 treatment, cryogenic grinding as well as incorporation of amine into the CB[6] cavity effectively helped to enhance the selective sequestration potential of the material. The increased adsorption values for the surface modified samples were mainly due to the availability of most of the CB[6] cavities for CO_2 adsorption compared to the unmodified sample. The increase in CO_2/N_2 selectivity value of 121.4 measured with the chemically (with ethanolamine) modified sample was found to be due to the chemical nature of the interaction between CO_2 and the amine group and the poor adsorption of N_2 in the amine rich modified material. The modified CB[6] material with its exceptional selectivity coupled with its inherent thermal stability and pore sizes compatible with gas molecular dimensions may find useful applications in various separation processes. The mechanism of the gas adsorption selectivity of modified CB[6] and methods to enhance it to the level of commercial adsorbents need further detailed investigations.

Abbreviations

CB[6]	Cucurbit[6]uril
CO_2	Carbon dioxide
EA	Ethanolamine
TZ2P	Triple-zeta doubly polarized

Conflicts of interest

There are no conflicts to declare.

Acknowledgements

We acknowledge the Council of Scientific and Industrial Research (CSIR), New Delhi, India, and Noritake Co. Limited, Aichi, Japan, for providing research facilities and financial support through the grant CLP 218739. JDG acknowledges the Australian Research Council for funding through the Discovery Programme, as well as the provision of computing resources through the National Computational Infrastructure (NCI) and the Pawsey Supercomputing Centre.

References

1 E. D. Bates, R. D. Mayton, I. Ntai and J. H. Davis, *J. Am. Chem. Soc.*, 2002, **124**(6), 926.
2 S. Diaz, J. Grime, J. Harris and E. McPherson, *Nature*, 1993, **364**(6438), 616.
3 W. C. Oechel, S. J. Hastings, G. Vourlrtis, M. Jenkins, G. Riechers and N. Grulke, *Nature*, 1993, **361**(6412), 520.
4 B. Wang, A. P. Cote, H. Furukawa, M. O'Keeffe and O. M. Yaghi, *Nature*, 2008, **453**(7192), 207.
5 P. Subha, B. N. Nair, P. Hareesh, A. P. Mohamed, T. Yamaguchi, K. Warrier and U. Hareesh, *J. Phys. Chem. C*, 2015, **119**(10), 5319.
6 P. Subha, B. N. Nair, P. Hareesh, A. P. Mohamed, T. Yamaguchi, K. Warrier and U. Hareesh, *J. Mater. Chem. A*, 2014, **2**(32), 12792.
7 N. MacDowell, N. Florin, A. Buchard, J. Hallett, A. Galindo, G. Jackson, C. S. Adjiman, C. K. Williams, N. Shah and P. Fennell, *Energy Environ. Sci.*, 2010, **3**(11), 1645.
8 J. C. Hicks, J. H. Drese, D. J. Fauth, M. L. Gray, G. Qi and C. W. Jones, *J. Am. Chem. Soc.*, 2008, **130**(10), 2902.
9 A. Busch, Y. Gensterblum, B. M. Krooss and N. Siemons, *Int. J. Coal Geol.*, 2006, **66**(1), 53.
10 R. Banerjee, H. Furukawa, D. Britt, C. Knobler, M. O'Keeffe and O. M. Yaghi, *J. Am. Chem. Soc.*, 2009, **131**(11), 3875.
11 R. Wang, D. Li and D. Liang, *Chem. Eng. Process.*, 2004, **43**(7), 849.
12 S. M. R. Razavi, A. Marjani and S. Shirazian, *Transp. Porous Media*, 2015, **106**(2), 323.
13 P. Li, B. Ge, S. Zhang, S. Chen, Q. Zhang and Y. Zhao, *Langmuir*, 2008, **24**(13), 6567.
14 F. Bougie, I. Iliuta and M. C. Iliuta, *Chem. Eng. Sci.*, 2015, **123**, 255.
15 M. Plaza, C. Pevida, A. Arenillas, F. Rubiera and J. Pis, *Fuel*, 2007, **86**(14), 2204.
16 M. T. Ho, G. W. Allinson and D. E. Wiley, *Ind. Eng. Chem. Res.*, 2008, **47**(14), 4883.
17 J. D. Figueroa, T. Fout, S. Plasynski, H. McIlvried and R. D. Srivastava, *Int. J. Greenhouse Gas Control*, 2008, **2**(1), 9.
18 D. Aaron and C. Tsouris, *Sep. Sci. Technol.*, 2005, **40**(1–3), 321.
19 X. Yan, L. Zhang, Y. Zhang, G. Yang and Z. Yan, *Ind. Eng. Chem. Res.*, 2011, **50**(6), 3220.
20 A. B. Rao and E. S. Rubin, *Environ. Sci. Technol.*, 2002, **36**(20), 4467.
21 T. C. Merkel, H. Lin, X. Wei and R. Baker, *J. Membr. Sci.*, 2010, **359**(1), 126.
22 V. Zelenak, M. Badanicova, D. Halamova, J. Cejka, A. Zukal, N. Murafa and G. Goerigk, *Chem. Eng. J.*, 2008, **144**(2), 336.
23 Z. Xiang and D. Cao, *J. Mater. Chem. A*, 2013, **1**(8), 2691.
24 K. Sumida, D. L. Rogow, J. A. Mason, T. M. McDonald, E. D. Bloch, Z. R. Herm, T.-H. Bae and J. R. Long, *Chem. Rev.*, 2011, **112**(2), 724.
25 H. R. Moon, D.-W. Lim and M. P. Suh, *Chem. Soc. Rev.*, 2013, **42**(4), 1807.
26 J. An, S. J. Geib and N. L. Rosi, *J. Am. Chem. Soc.*, 2009, **132**(1), 38.
27 P. Sudip, S. Mandal and P. K. Chattaraj, *J. Phys. Chem. B*, 2015, **119**(34), 10962.
28 P. Sudip, S. Mandal and P. K. Chattaraj, *New J. Chem.*, 2013, **37**, 2492.
29 D. Chakraborty, P. Sudip and P. K. Chattaraj, *Theor. Chem. Acc.*, 2016, **135**, 119.

30 S. Mandal, P. Sudip, D. Deb, S. Giri, S. Duley, S. Radenkovic, D. L. Cooper, P. Bultinck, A. Anoop, M. Bhattacharjee and P. K. Chattaraj, *Int. J. Quantum Chem.*, 2015, **115**, 1501.
31 J. Tian, S. Ma, P. K. Thallapally, D. Fowler, B. P. McGrail and J. L. Atwood, *Chem. Commun.*, 2011, **47**(27), 7626.
32 N. I. Saleh, A. L. Koner and W. M. Nau, *Angew. Chem.*, 2008, **120**(29), 5478.
33 A. Ol'ga, D. G. Samsonenko and V. P. Fedin, *Russ. Chem. Rev.*, 2002, **71**(9), 741.
34 S. Lim, H. Kim, N. Selvapalam, K. J. Kim, S. J. Cho, G. Seo and K. Kim, *Angew. Chem.*, 2008, **120**(18), 3400.
35 J. W. Lee, S. Samal, N. Selvapalam, H.-J. Kim and K. Kim, *Acc. Chem. Res.*, 2003, **36**(8), 621.
36 K. Kim, N. Selvapalam and D. H. Oh, *J. Inclusion Phenom. Macrocyclic Chem.*, 2004, **50**(1–2), 31.
37 W. S. Jeon, K. Moon, S. H. Park, H. Chun, Y. H. Ko, J. Y. Lee, E. S. Lee, S. Samal, N. Selvapalam and M. V. Rekharsky, *J. Am. Chem. Soc.*, 2005, **127**(37), 12984.
38 H. Kim, Y. Kim, M. Yoon, S. Lim, S. M. Park, G. Seo and K. Kim, *J. Am. Chem. Soc.*, 2010, **132**(35), 12200.
39 X.-L. Ni, X. Xiao, H. Cong, Q.-J. Zhu, S.-F. Xue and Z. Tao, *Acc. Chem. Res.*, 2014, **47**(4), 1386.
40 K. Kim, N. Selvapalam, Y. H. Ko, K. M. Park, D. Kim and J. Kim, *Chem. Soc. Rev.*, 2007, **36**(2), 267.
41 R. Vaidhyanathan, S. S. Iremonger, G. K. Shimizu, P. G. Boyd, S. Alavi and T. K. Woo, *Angew. Chem., Int. Ed.*, 2012, **51**(8), 1826.
42 J. Wang, L. Huang, R. Yang, Z. Zhang, J. Wu, Y. Gao, Q. Wang, D. O'Hare and Z. Zhong, *Energy Environ. Sci.*, 2014, **7**(11), 3478.
43 G. Qi, Y. Wang, L. Estevez, X. Duan, N. Anako, A.-H. A. Park, W. Li, C. W. Jones and E. P. Giannelis, *Energy Environ. Sci.*, 2011, **4**(2), 444.
44 N. Minju, P. Abhilash, B. N. Nair, A. P. Mohamed and S. Ananthakumar, *Chem. Eng. J.*, 2015, **269**, 335.
45 M. M. Maroto-Valer, C. Song and Y. Soong, *Springer Science & Business Media*, 2012.
46 H. Y. Huang, R. T. Yang, D. Chinn and C. L. Munson, *Ind. Eng. Chem. Res.*, 2003, **42**(12), 2427.
47 M. Gray, Y. Soong, K. Champagne, J. Baltrus, R. Stevens, P. Toochinda and S. Chuang, *Sep. Purif. Technol.*, 2004, **35**(1), 31.
48 P. Sudip, R. Saha, S. Mandal, S. Mondal, A. Gupta, M. A. Fernández-Herrera, G. Merino and P. K. Chattaraj, *J. Phys. Chem. C*, 2016, **120**(26), 13911.
49 N. S. Venkataramanan and A. Suvitha, *J. Phys. Chem. B*, 2017, **121**(18), 4733.
50 B. R. Strazisar, R. R. Anderson and C. M. White, *Energy Fuels*, 2003, **17**(4), 1034.
51 F. Karadas, M. Atilhan and S. Aparicio, *Energy Fuels*, 2010, **24**(11), 5817.
52 T. Filburn, J. Helble and R. Weiss, *Ind. Eng. Chem. Res.*, 2005, **44**(5), 1542.
53 D. Camper, J. E. Bara, D. L. Gin and R. D. Noble, *Ind. Eng. Chem. Res.*, 2008, **47**(21), 8496.
54 J. VandeVondele, M. Krack, F. Mohamed, M. Parrinello, T. Chassaing and J. Hutter, *Comput. Phys. Commun.*, 2005, **167**(2), 103.
55 S. Goedecker, M. Teter and J. Hutter, *Phys. Rev. B: Condens. Matter Mater. Phys.*, 1996, **54**(3), 1703.
56 J. P. Perdew, K. Burke and M. Ernzerhof, *Phys. Rev. Lett.*, 1996, **77**(18), 3865.
57 S. Grimme, J. Antony, S. Ehrlich and H. Krieg, *J. Chem. Phys.*, 2010, **132**(15), 154104.
58 W. Freeman, W. Mock and N. Shih, *J. Am. Chem. Soc.*, 1981, **103**(24), 7367.
59 J. Tian, J. Liu, J. Liu and P. K. Thallapally, *CrystEngComm*, 2013, **15**(8), 1528.
60 B. Yang, L.-M. Zheng, Z.-Z. Gao, X. Xiao, Q.-J. Zhu, S.-F. Xue, Z. Tao, J.-X. Liu and G. Wei, *J. Org. Chem.*, 2014, **79**, 11194.
61 X. Cui, W. Zhao, K. Chen, X.-L. Ni, Y.-Q. Zhang and Z. Tao, *Chem. – Eur. J.*, 2017, **23**, 2759.
62 T. M. McDonald, J. A. Mason, X. Kong, E. D. Bloch, D. Gygi, A. Dani, V. Crocellà, F. Giordanino, S. O. Odoh and W. S. Drisdell, *Nature*, 2015, **519**(7543), 303.
63 C. Gebald, *Development of amine-functionalized adsorbent for carbon dioxide capture from atmospheric air*, PhD dissertation, ETH Zurich, Diss. ETH No. 21853, 2014.